If the new variable $x = kr$ with $k^4 = \rho\omega^2/D_r$ is introduced and W assumed as

$$W \alpha \left[R_m(X) \begin{matrix}\cos\\ \sin\end{matrix} m\theta \right] e^{i\omega t} = \left\{ \left[\sum_{n=0}^{\infty} A_{m,n} x^{m+n} \right] \begin{matrix}\cos\\ \sin\end{matrix} m\theta \right\} e^{i\omega t} \tag{5}$$

Eq. (4) yields the following recurrence relation for the coefficients $A_{m,n}$:

$$A_{m,n} = \frac{A_{m,(n-4)}}{(m+n)(m+n-2)[(m+n-1)^2 - \beta] + m^2[(m^2-2)\beta - 2(\alpha+2\gamma)(m+n-1)^2]} \tag{6}$$

The axisymmetric modes corresponds to $m = 0$. In view of the recurrence relations (6), the function R_m can be written in terms of the first four coefficients, namely, $A_{m,0}$, $A_{m,1}$, $A_{m,2}$, and $A_{m,3}$. At the center of the plate ($r = 0$) the two conditions to be enforced are that for all values of m: 1) the left-hand side of Eq. (4) must vanish, and 2) the moments must be finite. These conditions lead to $A_{m,1} = A_{m,3} = 0$ so that the function $R_m(X)$ becomes

$$R_m = A_{m,0} \sum_{j=0,4,8}^{\infty} C_{m,j} X^{m+j} + A_{m,2} \sum_{j=0,4,8}^{\infty} D_{m,j} X^{m+j+2} \tag{7}$$

where $C_{m,j} = A_{m,j}/A_{m,0}$ and $D_{m,j+2} = A_{m,j+2}/A_{m,2}$. Equation (6), when specialized for the isotropic case [$\alpha = \nu =$ Poisson's ratio, $\beta = 1$ and $(\alpha + 2\gamma) = 1$], reduces to

$$A_{m,n} = A_{m,(n-4)}/n(n-2)(2m+n)(2m+n-2) \tag{8}$$

With the coefficients given by Eq. (8), the series for R_m [Eq. (7)] can be shown to be a linear combination of the Bessel functions $J_m(X)$ and $I_m(X)$. Therefore, for the isotropic plate, the solution reduces to that given by Rayleigh[2] and by Morse.[3]

When the boundary conditions $W = \partial W/\partial r = 0$ at the edge $r = a$ ($X = ka = X_1$) for a clamped plate or $W = M_r = 0$ at $r = a$ for a simply supported plate are enforced, Eq. (7) yields the following characteristic equations for the determination of the natural frequencies:

$$\left[\sum_j C_{m,j} X_1^{m+j}\right]\left[\sum_j (m+j+2) D_{m,j+2} X_1^{m+j+1}\right] - \left[\sum_j (m+j) C_{m,j} X_1^{m+j-1}\right]\left[\sum_j D_{m,j+2} X_1^{m+j+2}\right] = 0 \tag{9}$$

$$\left[\sum_j C_{m,j} X_1^{m+j}\right]\left[\sum_j \{(m+j+2)(m+j+1+\alpha) - \alpha m^2\} D_{m,j+2} X_1^{m+j}\right] - \left[\sum_j \{(m+j)(m+j-1+\alpha) - \alpha m^2\} C_{m,j} X_1^{m+j-2}\right]\left[\sum_j D_{m,j+2} X_1^{m+j+2}\right] = 0 \tag{10}$$

If the infinite series appearing in the foregoing equations is restricted to include terms up to the power $(2m + 4)$, a first approximation for the values of (ka) corresponding to the lowest frequencies are obtained as

$$(ka)^4_{\text{clamped}} = 1/(C_{m,4} - 3D_{m,6}) \tag{11}$$

$$(ka)^4_{s,s} = \frac{2m+1+\alpha}{2m+5+\alpha}(ka)^4_{\text{clamped}} \tag{12}$$

For the isotropic plate the foregoing equations simplify to

$$(ka)^4_{\text{clamped}} = (m+1)(m+2)(m+3)\cdot 2^4$$
$$(ka)^4_{ss} = \frac{2m+1+\nu}{2m+5+\nu}(ka)^4_{\text{clamped}} \tag{13}$$

Using Eqs. (13) with $\nu = \frac{1}{3}$, values of (ka) for $m = 0$, 1, and 2 are, respectively, 3.13, 4.43, and 5.57 for the clamped plate and 2.21, 3.63, and 4.84 for the simply supported plate. These values obtained as first approximations agree well with those obtained from the solution in terms of the Bessel functions. If for $m = 0$, a second approximation involving terms up to the eighth power in (ka) is considered for the clamped plate, the values of the first two frequencies are obtained from $(ka) = 3.198$ and 5.855, whereas the solution to the characteristic equation in terms of the Bessel functions yields $(ka) = 3.2$ and $(ka) \cong 6.3$.[2] For $m = 0$, for the orthotropic clamped plate, the first approximation [Eq. (11)] gives, $(ka)^4 = (9 - \beta)(25 - \beta)/2$, from which it can be concluded that for $\beta \gtrless 1$, $(ka)^4 \lessgtr 96$.

References

[1] Timoshenko, S. and Woinowsky-Krieger, S., *Theory of Plates and Shells* (McGraw-Hill Book Co., Inc., New York, 1959), 2nd ed., Chap. XI, p. 364.

[2] Lord Rayleigh, *The Theory of Sound* (Dover Publications, New York, 1945), Vol. 1, 2nd ed., Chap. X, pp. 360–367.

[3] Morse, P. M., *Vibration and Sound* (McGraw-Hill Book Co., Inc., New York, 1948), 2nd ed., Chap. V, p. 210.

A Heat-Transfer Criterion for the Detection of Incipient Separation in Hypersonic Flow

DAVID A. NEEDHAM*

Imperial College, London, England

PREVIOUS studies of flow separation resulting from shock-wave boundary-layer interaction in supersonic flow have encountered the difficulty of detecting incipient separation. When the region of separation is relatively large, the flow pattern exhibits the characteristic shock wave from the separation point visible upstream of the agency provoking separation. The pressure distribution then exhibits the familiar plateau pressure occurring between separation and reattachment. The first appearance of a knee in the pressure distribution, generating three points of inflexion instead of the one typical of an attached flow, has been used by many investigators to indicate the onset of separation. The applicability of this criterion to high Mach number studies conducted in intermittent facilities with very short running times is doubtful on account of the low accuracy of pressure measurements. Either an alternative or additional criterion is desirable.

In a current research program being conducted in the Imperial College Hypersonic Gun Tunnel, the separation of the flat plate laminar boundary layer due to the interaction with either an externally generated oblique shock wave or a wedge compression-corner is being investigated at a Mach number of 10. As a precursor to the main part of the work, measurements of the heat-transfer rates in the interaction region were made using thin-film resistance thermometer gages.†

Pressure measurements obtained recently for identical configurations have substantiated the results of the heat-transfer work. In Fig. 1, the pressure- and heat-transfer distributions obtained on the wedge compression-corner model for various wedge angles are presented together with the corresponding schlieren photographs of the flow in the neighborhood of the corner. In Fig. 1a, the flow is fully attached with

Received December 2, 1964.

* Research Assistant, Department of Aeronautics. Associate Member AIAA.

† This work was performed conjointly by the present author and M. S. Holden, and is reported by the latter author in Ref. 1.

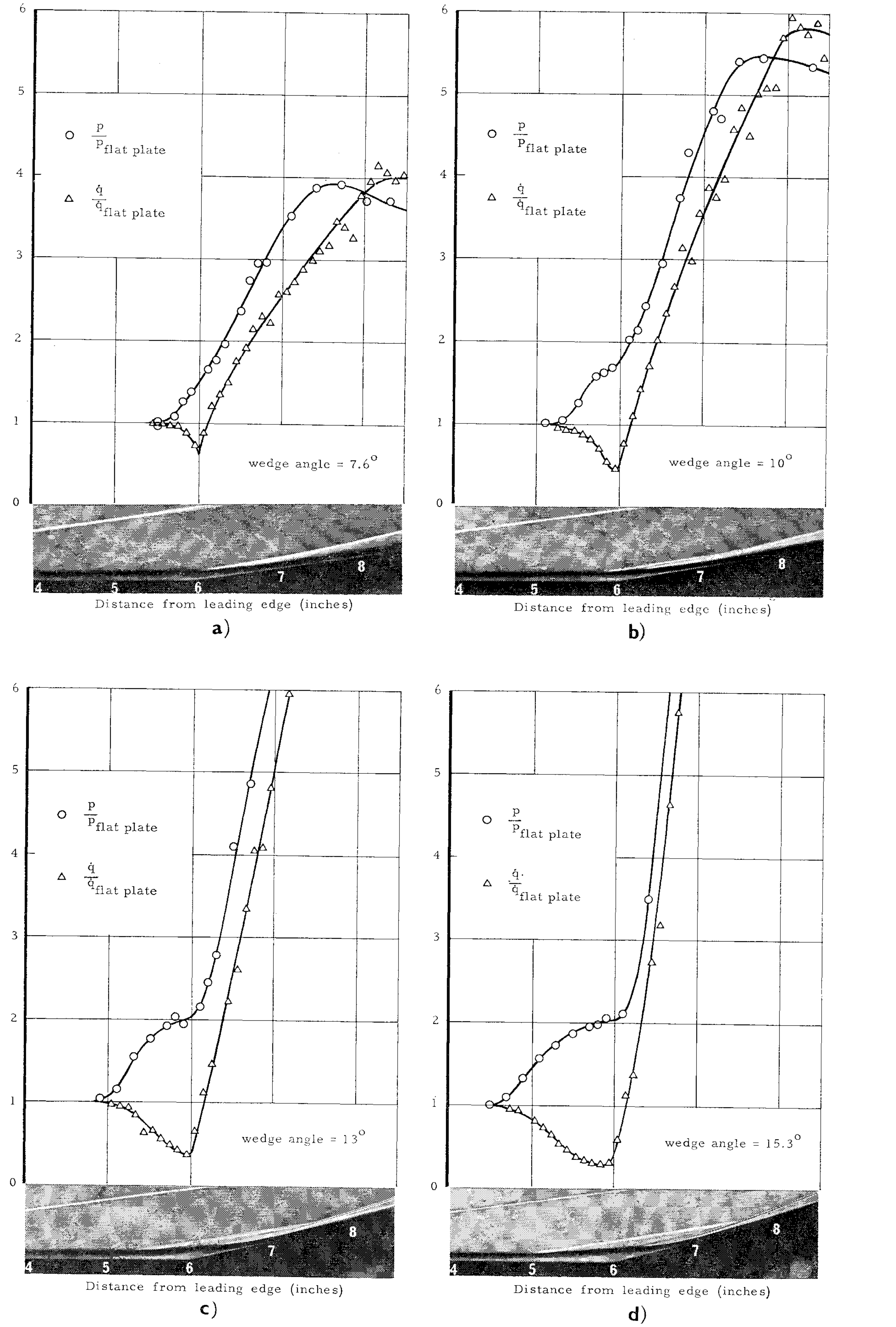

Fig. 1 Pressure- and heat-transfer distributions and schlieren photographs of flow over a compression corner at various wedge angles. $M_\infty = 9.7$, $Re_\infty = 1.48 \times 10^5$/in.

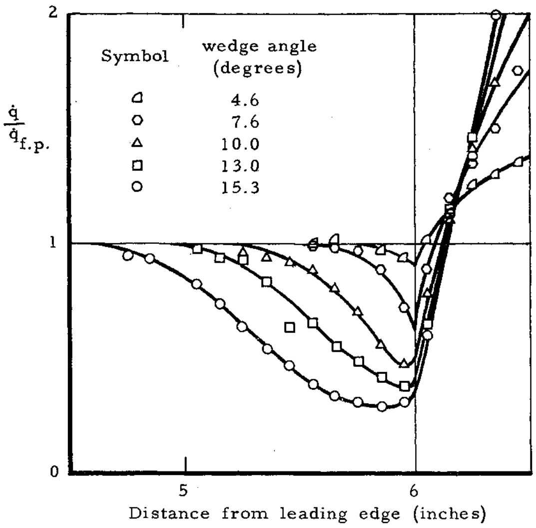

Fig. 2 Heat-transfer distributions for attached and separated flows.

a single shock wave visible at the outer edge of the boundary layer downstream of the corner. The pressure distribution has a single point of inflexion whereas the heat-transfer distribution exhibits a cusp-like minimum at the corner. The decrease in heat transfer ahead of the corner coincides with the initial rise in pressure resulting from the upstream influence of the wedge. Downstream of the corner the heat-transfer rate rises steeply in the region of high pressure gradient, reaching a maximum value just downstream of the peak pressure. As the wedge angle is increased, a small region of flow separation is formed in the corner, as in Fig. 1b, in which two shock waves are visible: one plane oblique shock generated by the boundary-layer separation point upstream of the corner, and a second concave curving shock just downstream of the corner in the reattachment region. The pressure distribution then exhibits a knee just upstream of the corner and the heat transfer is seen to develop a smooth minimum with a continuously changing gradient instead of the cusp typical of the attached flow. As the wedge angle is increased further, as in Figs. 1c and 1d, the size of the separated region grows as the separation point moves upstream, and the knee in the pressure distribution broadens, although the plateau pressure characteristic of fully separated flows is only just attained at the largest wedge angle tested. The heat-transfer minimum retains the smooth curvature and broadens out as the separation point moves upstream. This general trend in heat transfer has previously been observed by Miller, Hijman and Childs,[2] although the detailed structure in large regions of separation appears to differ from the findings of this investigation.

The change in form of the heat-transfer distribution between attached and separated flows is best seen in Fig. 2 where the results obtained for wedge angles from 4.6° to 15.3° are superimposed. From these observations it appears that incipient separation occurs for this case between 7.6° and 10.0° and probably closer to the former wedge angle. An estimate of the wedge angle for incipient separation obtained from an extrapolation of a plot of separation length against wedge angle indicated a value of 8°.

The heat-transfer criterion for the detection of incipient separation described in this note has been used recently by Stollery[3] in a study of wedge separation at $M = 14$. In the current program conducted by the author, the heat-transfer criterion has been used to supplement the evidence of incipient separation obtained from pressure measurements and schlieren photographs However, it is believed that in short running time, low-density hypersonic facilities, the faster response of heat-transfer gages, and the high instrumentation density possible with the thin-film technique will render this criterion for the detection of incipient separation of greater value than the equivalent one based on pressure measurements.

References

[1] Holden, M. S., "Heat transfer in separated flow," Ph.D. Thesis, University of London, London (1964).

[2] Miller, D. S., Hijman, R., and Childs, M. E., "Mach 8 to 22 studies of flow separations due to deflected control surfaces," AIAA J. 2, 312–321 (1964).

[3] Stollery, J. L. and Holden, M. S., "Incipient separation of a laminar boundary layer in hypersonic flow," Cornell Aeronautical Lab. Rept. (to be published).

Hall Potentials in Nonequilibrium MHD Generators

Arthur Sherman*
General Electric Company, Valley Forge, Pa.

Introduction

Based largely on an anticipated need for large quantities of electrical power (megawatt level) for space missions, there is a considerable interest in MHD generators operating at gas temperatures consistent with near future nuclear reactor technology. Since these temperatures are quite low compared to those necessary for thermal ionization of the gas, one must rely on some form of nonequilibrium ionization. Accordingly, experiments[1, 2] have been designed to evaluate the feasibility of creating the desired nonequilibrium state solely by use of the self-induced electric field in the MHD generator. In both of these, it has been demonstrated that such an effect does exist.

At the same time, however, it has been shown that lower Hall voltages than predicted are obtained experimentally. There are several possible explanations for this, all depending on the fact that the plasma is, or is intended to be, in a nonequilibrium state. One explanation suggests that shorting along the segmented electrodes may be causing the low voltages.[3] It will be the purpose of the present note to explore an alternate possibility, which involves shorting along the insulator surfaces.

The essential question to be asked is: Why should one expect the open-circuited Hall voltage to be

$$E_x = \omega\tau(E_y - uB_z) \tag{1}$$

where u is the flow velocity in the x direction, ω is the electron cyclotron frequency, and τ is the mean time between collisions? For the simplest case, where σ is constant and $\mathbf{v} = (u, 0, 0)$ with u constant, the generalized Ohm's law[4] yields Eq. (1). If additional complexity is admitted, velocity profiles may exist so that $\mathbf{v} = (u, v, 0)$ where both may vary in a direction normal to the insulator surfaces, and v is a cross flow. Even in this far more complicated situation it has been found[5] that Eq. (1) is still valid if u is taken to be the average value. This is true in spite of the fact that *axial currents do flow.*

It will be the purpose of the present note to consider further the validity of Eq. (1) when not only velocity profiles are included, but the nonequilibrium effect is also allowed for.

Received December 30, 1964. The author wishes to express his appreciation to R. Casten for assisting with the numerical computations. This work was supported by the U. S. Air Force Office of Scientific Research, Contract No. AF 49(638)-1465.

* Manager, MHD Power Generation Laboratory, Space Sciences Laboratory. Associate Fellow Member AIAA.